ACS APPLIED MATERIALS & INTERFACES

Research Article

www.acsami.org

Well-Organized Meso-Macroporous TiO_2/SiO_2 Film Derived from Amphiphilic Rubbery Comb Copolymer

Harim Jeon,[†] Chang Soo Lee,[†] Rajkumar Patel,[‡] and Jong Hak Kim*,[†]

[†]Department of Chemical and Biomolecular Engineering, Yonsei University, 262 Seongsanno, Seodaemun-gu, Seoul 120-749, South Korea

[‡]Division of Physics & Semiconductor Science, Dongguk University, Seoul 100-715, South Korea

Supporting Information

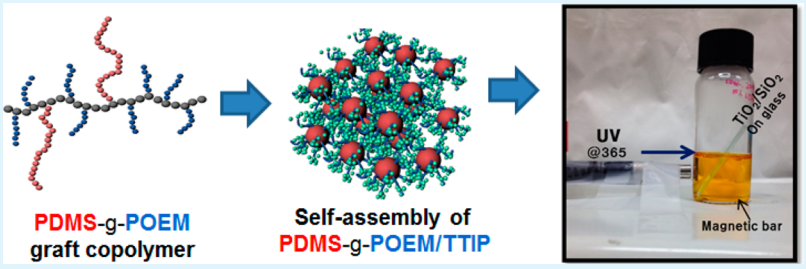

ABSTRACT: We report the facile synthesis of a well-organized meso-macroporous TiO_2/SiO_2 thin film with high porosity and good interconnectivity from a binary mixture (i.e., titania precursor and polymer template). Our process is based on self-assembly of the amphiphilic rubbery comb copolymer, poly(dimethylsiloxane)-*g*-poly(oxyethylene methacrylate) (PDMS-*g*-POEM) with titanium tetraisopropoxide (TTIP). SiO_2 is self-provided by thermal oxidation of PDMS chains during calcination under air. The selective, preferential interaction between TTIP and the hydrophilic POEM chains was responsible for the formation of well-organized TiO_2/SiO_2 films, as supported by transmission electron microscopy, scanning electron microscopy, X-ray photospectroscopy, and X-ray diffraction analyses. We investigated in detail the effect of precursor content, solvent type, and polymer concentration on thin film morphology. Photodegradation of methyl orange by the well-organized meso-macroporous TiO_2/SiO_2 film was greater than that of a dense TiO_2 film prepared without PDMS-*g*-POEM as well as a SiO_2-etched TiO_2 film. These results indicate that the well-organized structure and SiO_2 doping of the TiO_2 film play a pivotal role in enhancing its photocatalytic properties.

KEYWORDS: *SiO_2, TiO_2, thin film, comb copolymer, photocatalytic property*

INTRODUCTION

Synthesis of porous materials has drawn considerable academic interest since an organic soft template made of amphiphilic surfactants was used to prepare ordered meso-macroporous silicates with pore diameters of 2−50 nm in the 1990s.[1] Porous structures have a large internal surface area per weight and therefore offer high accessibility and diffusivity to guest molecules, allowing them to penetrate through pores, which in turn enhances device efficiency and chemical reactions. Titania (TiO_2) is one of the most promising materials in energy and environmental fields due to its wide band gap energy, nontoxicity, chemical stability, low cost, and ease of synthesis into various structures at the nano scale.[2−5] In particular, better performances have been obtained in various applications, such as photocatalysis, drug-delivery, chemical sensors, and photovoltaic cells, using well-defined porous TiO_2 structures than dense, nonporous structures because interacting molecules have greater surface access in porous structures.[6−8] Therefore, considerable research effort has been devoted to developing effective methods to precisely control the formation of well-defined porous structures (i.e., the size and connectivity of pores, pore wall thickness, degree of ordering, bimodal/hierarchical porous structure, etc).

Evaporation-induced self-assembly (EISA) is a rapid, facile, and versatile approach first described by Brinker et al.[9] for the preparation of highly ordered, robust, and porous TiO_2 films. In EISA, characteristics of porosity can be controlled by careful adjustment of processing parameters, including the nature of the surfactant and precursor, molar ratio of precursor to polymer, relative humidity, concentration of polymer solution, reaction time of the sol−gel process, calcination temperature, and dwelling time. The most common polymers used in EISA are commercially available Pluronic block copolymers, namely, P123 ($PEO_{20}PPO_{70}PEO_{20}$) and F127 ($PEO_{106}PPO_{70}PEO_{106}$) with average molecular weights of 5800 and 12500 g/mol, respectively, where P and F stand for the physical states of paste and flake, respectively.[10] In general, Pluronic-type block copolymers generate mesopores from 5 to 9 nm with a wall

Received: February 3, 2015
Accepted: March 24, 2015
Published: March 24, 2015

DOI: 10.1021/acsami.5b01010
ACS Appl. Mater. Interfaces 2015, 7, 7767−7775

thickness of 5−9 nm; however, this is too small for some applications, such as solid-state dye-sensitized solar cells, in which pore infiltration by solid electrolytes is of critical importance. Furthermore, because of the low thermal stability of Pluronic copolymers, the resulting TiO_2 mesostructures often suffer from short-range pore ordering and pore wall collapse during thermal treatment at around 300−400 °C.

Alternative polymers used in EISA are high molecular weight (>20000 g/mol) amphiphilic block copolymers that microphase-separate into hydrophilic domains and hydrophobic domains. Use of block copolymer results in TiO_2 films with large pore sizes and thick walls with enhanced ordering of porous structures spanning several orders of magnitude in length. For example, Cheng et al.[11] used polystyrene-*b*-poly(ethylene oxide) (PS-*b*-PEO, 19000g/mol) diblock copolymer as a structure-directing agent together with titanium tetraisopropoxide (TTIP), 1,4-dioxane, and HCl. They reported the formation of various morphologies of anatase TiO_2, such as nanowires, flake-like aggregates, worm-like aggregates, foam-like aggregates, and nanodoughnuts by simply changing the relative weight fractions of 1,4-dioxane, HCl, and TTIP. Furthermore, a triblock copolymer composed of polystyrene-*b*-poly(vinylpyridine)-*b*-poly(ethylene oxide) (PS-*b*-PVP-*b*-PEO) was employed to form a meso-macroporous anatase TiO_2 film with a pore size of 40−50 nm and wall thickness of 10−40 nm.[12,13] The different tree blocks had different roles in sol−gel chemistry. In another study, a poly(ethylene-*co*-butylene)-*b*-poly(ethylene oxide) block polymer was used to form a three-dimensional cubic meso-macroporous structure. This structure showed excellent thermal stability at 700 °C and had an intact porous architecture due to the presence of anatase TiO_2 with 100% crystallinity.[14] However, these high molecular weight amphiphilic block copolymers are expensive and hard to synthesize in the laboratory due to their high sensitivity to impurities such as O_2 or water.

TiO_2/SiO_2 mixed oxides have been investigated as materials that can potentially enhance the photocatalytic activity of TiO_2.[15−19] Although SiO_2 is known to have poor photoactivity, addition of SiO_2 to TiO_2 could have several benefits, such as preferential adsorption of specific materials (e.g., rhodamine-6G) in the vicinity of the photoactive center,[16] an increase in specific surface area by retarding the crystal size growth of TiO_2,[17] the formation of Ti−O−Si heterolinkages as stronger Brønsted acid sites where tetrahedrally coordinated silica is molecular-scale mixed with the octahedral titania matrix,[18] and suppression of phase transformation from anatase to rutile at elevated temperatures up to 1000 °C.[19] Despite many reports on the use of TiO_2/SiO_2 mixed oxides in various applications, most studies have used a Si inorganic precursor. For the preparation of well-ordered TiO_2/SiO_2 thin films, three components, namely, a Ti inorganic precursor, Si inorganic precursor, and organic polymer template, are required.

Here, we report cheap, facile synthesis of a well-organized meso-macroporous TiO_2/SiO_2 mixed oxide thin film in the absence of a Si inorganic precursor. Our process is based on self-assembly of the amphiphilic rubbery comb copolymer poly(dimethylsiloxane)-*graft*-poly(oxyethylene methacrylate) (abbreviated to PDMS-*g*-POEM) with TTIP, an inorganic precursor of TiO_2. SiO_2 formation in the film stemmed from thermal oxidation of PDMS chains during calcination in air. The pore size and porosity of the TiO_2/SiO_2 films are controllable due to cooperative assembly of PDMS-*g*-POEM and TTIP into large micelles in a polar solvent. Materials were characterized using Fourier transformed infrared spectroscopy (FT-IR), energy-filtering transmission electron microscopy (EF-TEM), thermogravimetric analysis (TGA), field-emission scanning electron microscopy (FE-SEM), high resolution transmission electron microscopy (HRTEM), X-ray photospectroscopy (XPS), and X-ray diffraction (XRD) analyses. The effects of precursor content and polymer concentration are discussed in detail. Photodegradation of methyl orange by the well-organized meso-macroporous TiO_2/SiO_2 film was also investigated and compared with that of a dense TiO_2 film prepared without PDMS-*g*-POEM as well as a SiO_2-etched TiO_2 film.

EXPERIMENTAL SECTION

Materials. Monomethacryloxypropyl monobutyl-terminated poly(dimethylsiloxane) (PDMS-mMA) with a viscosity of 135−220 cSt was obtained from Gelest Incorporated. Poly(oxyethylene) methyl ether methacrylate (POEM) with a molecular weight of 500 g/mol, 2,2′-azobis(2-methylpropionitrile) (AIBN, 98%), methyl orange (MO), and ethyl acetate (ACS grade) were purchased from Sigma-Aldrich. Diethyl ether, hexane, toluene, tetrahydrofuran, isopropyl alcohol, ethanol, methanol, and HCl (37%) aqueous solution of HPLC grade were obtained from Ducksan Incorporated. All reagents were used without further purification.

Synthesis of PDMS-*g*-POEM Comb Copolymer. The amphiphilic rubbery comb copolymer poly(dimethylsiloxane)-*graft*-poly(oxyethylene) methacrylate (PDMS-*g*-POEM) was synthesized via free-radical polymerization in a batch reactor as shown in Scheme 1.

Scheme 1. Synthesis of PDMS-*g*-POEM Comb Copolymer

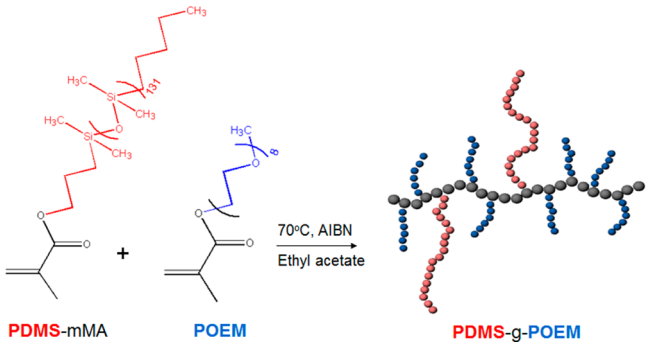

First, 12 mL of PDMS-mMA and 26 mL of POEM were added to 120 mL of ethyl acetate in a 250 mL round-bottom glass flask. Then, 12 mg of AIBN was added, and the mixture was stirred until a homogeneous and transparent solution was obtained. The flask was tightly sealed and purged with nitrogen for 1 h to remove oxygen in the solution, which deactivates radical polymerization. The flask was then placed in an oil bath at a temperature of 70 °C for 24 h under constant stirring with a magnetic bar. After the flask cooled down to room temperature, the polymer was precipitated in cold hexane three times and then dried in a vacuum oven at 50 °C for 1 day. The polymer was obtained as a white, opaque, sticky solid. The average molecular weight of PDMS-*g*-POEM comb copolymer was 14400 g/mol with a PDMS/POEM ratio of 1:1.5, as determined by gel permeation chromatography (GPC).

Preparation of aWell-Organized TiO_2/SiO_2 Film. First, 0.1 g of synthesized PDMS-*g*-POEM comb copolymer was dissolved in 1.9 g of ethanol to make a polymer solution at a concentration of 5 wt %. In a different vial, a TTIP sol was prepared by mixing TTIP, HCl (37%), and water drop by drop at a volume ratio of 2:1:1. It is important to add one drop of HCl at a time with an interval of ∼1−2 s to retard the rate of the condensation reaction. After 30 min, 0.075 mL of TTIP sol was slowly added to the polymer solution and stirred for 3 h. Adding

DOI: 10.1021/acsami.5b01010
ACS Appl. Mater. Interfaces 2015, 7, 7767−7775

TTIP sol to the polymer solution immediately induced phase separation from a transparent and dilute solution to a translucent and viscous gel, which indicated precipitation of the polymer out of the solution due to the introduction of water, which is a poor solvent for the polymer. However, after vigorous agitation by a magnetic bar at a high rpm, a transparent and homogeneous solution was finally prepared, indicating stabilization of the molecular arrangement. After aging at room temperature for 3 h, the solution was spread onto the substrate, fluorine-doped tin oxide coated glass (FTO glass) at 1500 rpm for 20 s using a spin-coater. The volatile ethanol evaporated during this process, but the optical transparency of the organic−inorganic hybrid structure in the water-enriched environment was maintained. Finally, a calcination process was performed at 500 °C for 1 h in static air to harden the frame into a higher crystalline inorganic phase and generate pores by removal of the copolymer as a result of oxidative thermal degradation. To compare photocatalytic efficiency of the meso-macroporous TiO_2/SiO_2 composite, a dense TiO_2 film was also prepared in the same way in the absence of PDMS-*g*-POEM. Moreover, the etched TiO_2 film was prepared by selectively etching the SiO_2 component in the meso-macroporous TiO_2/SiO_2 composite and dried in an oven at 50 °C. Silica (SiO_2) was eliminated by immersing the meso-macroporous TiO_2/SiO_2 composite film in 8 mol L^{-1} of NaOH aqueous solution at 50 °C for 10 h and rinsed away by washing with ethanol and water several times.

Characterization. Fourier-transform infrared spectroscopy (FT-IR) measurements were performed using an FT-IR spectrometer (Spectrum 100, PerkinElmer). The relative molecular weight and molecular weight distribution of the synthesized polymer were determined by gel permeation chromatography (GPC) calibrated against a series of polystyrene standards with tetrahydrofuran as the eluent at a flow rate of 1.0 mL min^{-1}. The synthesized polymer was filtered using a syringe-type commercial poly(vinylidene fluoride) membrane with the pore size of 450 nm to remove impurities before injection into GPC. Energy-filtering transmission electron microscopy (EF-TEM) was performed using a LIBRA 120 (Carl Zeiss) instrument at an accelerating voltage of 120 kV. For sample preparation for EF-TEM, a drop of 1 wt % polymer solution in ethanol was cast onto a carbon coated-TEM grid, and the solvent evaporated in an oven at 50 °C. Thermal stability of the synthesized polymer (10 mg) was examined by thermogravimetric analysis (TGA) (Q-5000 IR, TA Instruments, USA) at a heat ramping rate of 10 °C/min from ambient temperature to 600 °C under a constant flow rate of inert nitrogen or air. Field-emission scanning electron microscope images were taken using a SUPRA 55VP (Carl Zeiss, Germany). Sputtering of Pt onto the surface of TiO_2 was not necessary due to the semiconducting property of TiO_2. For TEM measurements, TiO_2 films were collected by scratching from the glass substrate and sonication for 20 min to disperse the particles homogeneously in ethanol. The resultant dispersion was dropped onto the surface of a carbon film-coated TEM grid and dried at 50 °C. Energy-dispersive X-ray spectroscopy was performed using an XFLASH detector 4070 (Bruker), and photoelectron spectroscopy measurements were performed by XPS (mono) with a monochromated AI Kα source (ARXPS, Thermo, U.K.). For XRD measurements,the PDMS-*g*-POEM thin film was prepared by casting the polymer solution onto a Teflon dish and drying at 50 °C overnight, followed by transfer to an XRD glass holder. Wide-angle X-ray diffraction patterns of the TiO_2 film on FTO were obtained from 10−80° by high resolution X-ray diffractometry (D8 Advance, Bruker, Germany).

Photocatalytic Performance. The photoactivity efficiency of the TiO_2/SiO_2 mixed oxide film templated by PDMS-*g*-POEM was investigated by determining the photobleaching rate of the organic dye methyl orange (MO) after UV radiation. For the effect of the porous structure of the TiO_2/SiO_2 mixed oxide film to be examined, two different control samples were prepared: dense TiO_2 and a silica-etched TiO_2 film. The dense TiO_2 film was prepared in the same way as the meso-macroporous TiO_2/SiO_2 mixed oxide film in the absence of PDMS-*g*-POEM. Silica-etched TiO_2 was prepared by post-etching of the meso-macroporous TiO_2/SiO_2 mixed oxide film with 8 M NaOH at 50 °C for 10 h followed by several rinses with water and ethanol. A spot mercury lamp (INNO cure 100N, lamp power: 80 W) with a UV intensity of ~2000 mW/cm^2 centered at 364 nm was used as a light source. Three types of films (1.5 cm (W) × 2.0 cm (L)) on glass were leaned against the wall of a 30 mL glass vial and immersed in 10 mL of MO aqueous solution at a concentration of 10 mg/L (3.06×10^{-5} M). Before irradiation with UV light, the mixtures were stabilized for 30 min in the dark to obtain an equilibrated adsorption concentration. The surfaces of the films were illuminated with UV light for 4 h with constant magnetic agitation. Photodegradation rates of MO by various thin films were compared by measuring the absorbance value of MO at 463 nm on a UV−vis spectrophotometer.

RESULT AND DISCUSSION

Characterization of PDMS-*g*-POEM Comb Copolymer. Amphiphilic PDMS-*g*-POEM copolymer was synthesized from two different monomethacylate-terminated macromonomers (PDMS-mMA and POEM) via free radical polymerization, which is a cheap and easy method to synthesize copolymers.[20] The solvent for free radical polymerization should meet several requirements, including good solubility of macromonomers. The solubility parameter (δ) is a good indicator of interactions between and miscibility of different materials. The solubility parameters of PDMS-mMA and POEM are ~7.3 and 9.7 $cal^{1/2}$ $cm^{-3/2}$, respectively.[21,22] Another requirement for the solvent is a high boiling point (bp) that exceeds the thermal decomposition temperature of the radical initiator (T_d = 65 °C for AIBN) and ease of precipitation of the synthesized polymer in a nonsolvent. Because of the large difference in polarity between PDMS-mMA and POEM, we selected a neutral solvent to dissolve both macromonomers homogeneously. Ethyl acetate (δ = 9.0, bp = 77 °C) was chosen in this system, but toluene (δ = 8.9, bp =111 °C) could be used for reaction temperatures above 95 °C. The solubility of the synthesized PDMS-*g*-POEM comb copolymer was tested with a wide solubility range of solvents, including diethyl ether (δ = 7.5), toluene (δ = 8.9), tetrahydrofuran (δ = 9.3), isopropyl alcohol (δ = 11.6), ethanol (δ = 12.7), methanol (δ = 14.5), and water (δ = 23.4) at a concentration of 10 wt %. Solubility tests revealed that the synthesized PDMS-*g*-POEM comb copolymer was soluble in a wide range of solvents from toluene to methanol; exceptions were extremely nonpolar and polar solvents, such as diethyl ether and water, respectively.

Successful synthesis of PDMS-*g*-PEOM comb copolymer was confirmed by FT-IR spectroscopy as shown in Figure 1a. The presence of methacrylate in POEM with a molecular weight of 500 g/mol was confirmed by the sharp peaks at 1717 and 1637 cm^{-1} caused by the stretching vibration of the carbonyl group (-C═O) in the ester and stretching unsaturated double bond (-C═C), respectively.[23] However, the presence of methacrylate in PDMS-mMA with a molecular weight of 10000 g/mol was not clearly observed due to the much lower concentration of terminal methacrylate groups than repeating units of PDMS. The peaks of PDMS-mMA at 1280 and 790 cm^{-1} are due to symmetric CH_3 deformation and $Si(CH_3)_2$ rocking, respectively.[24] The synthesized PDMS-*g*-POEM comb copolymer had a strong characteristic peak at 1028 cm^{-1} due to asymmetric stretching vibration of Si−O−Si.[24] A typical asymmetric ether (-O—) stretching peak was also observed at 1095 cm^{-1} for the PDMS-*g*-POEM copolymer. The carbonyl peak of ester in the methacrylate group also appeared at 1727 cm^{-1} in the PDMS-*g*-POEM copolymer, indicating that carbon double bonds were cleaved and that single bonds covalently linked POEM and PDMS-mMA. We attributed the slight peak shift from 1717 to 1727 cm^{-1} to weakened C═O bond strength in PDMS-*g*-

DOI: 10.1021/acsami.5b01010
ACS Appl. Mater. Interfaces 2015, 7, 7767−7775

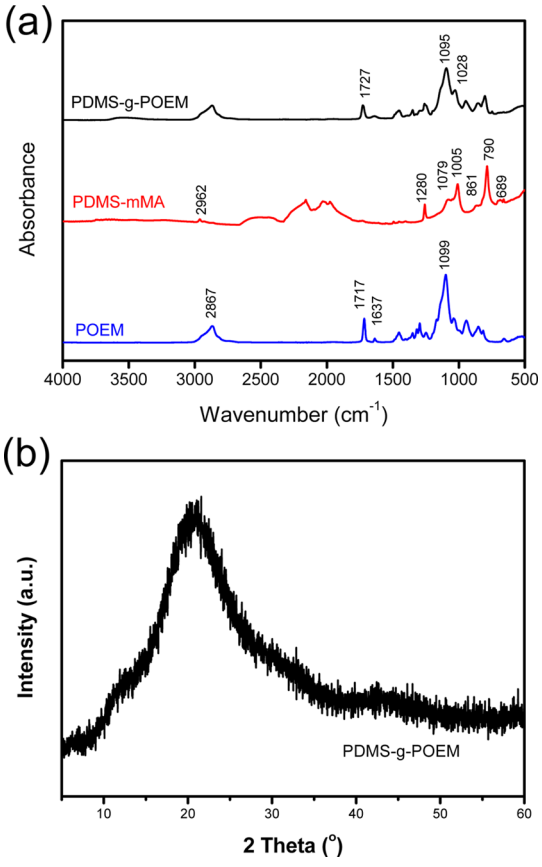

Figure 1. (a) FT-IR spectra of POEM macromonomer, PDMS-mMA macromonomer, and PDMS-*g*-POEM comb copolymer. (b) XRD pattern of PDMS-*g*-POEM comb copolymer.

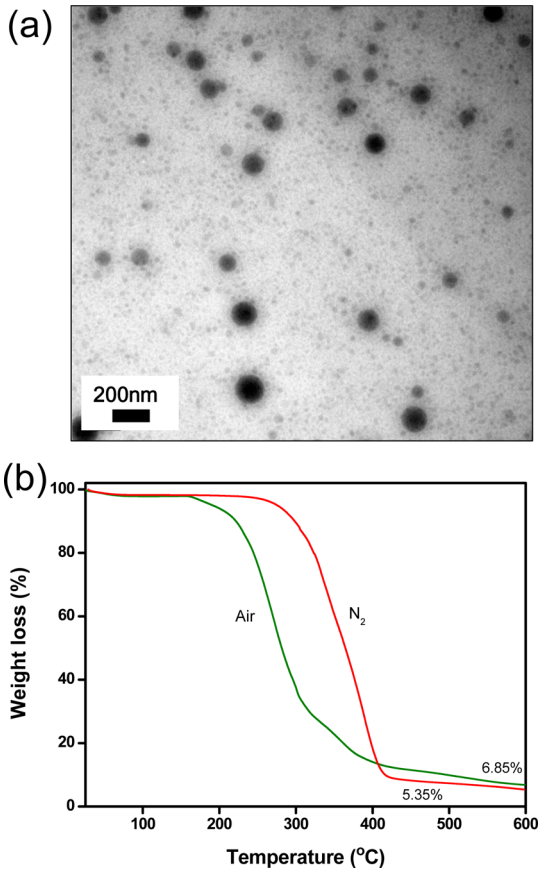

Figure 2. (a) TEM image of PDMS-*g*-POEM comb copolymer prepared using ethanol as a solvent. (b) TGA curves of PDMS-*g*-POEM comb copolymer under nitrogen and air.

POEM compared to the POEM macromonomer due to steric interference by the PDMS chains of secondary bonding interactions among POEM interchains/intrachains.

The microstructure of synthesized PDMS-*g*-POEM comb copolymer was characterized using XRD analysis, which has been established as a powerful tool to investigate structural changes in polymers. The intensity of X-ray scattering for the PDMS-*g*-POEM copolymer is plotted against the diffraction angle (2θ) in Figure 1b. The PDMS-*g*-POEM comb copolymer had an amorphous nature with a broad peak centered at a diffraction angle of 20.8°. Additional weak peaks were also observed at 31.9° and 43.2°. Using the Bragg equation, the interchain *d*-spacing was calculated to be 4.3, 2.8, and 2.1 Å, respectively. These results indicate that the PDMS-*g*-POEM comb copolymer was a structureless, randomly moving coil state with high mobility, which allowed it to interact effectively with the metal oxide precursor to form a robust metal oxide thin film after calcination.

The self-arrangement of PDMS-*g*-POEM comb copolymer into uniform spherical micelles in a polar solvent, such as ethanol, was proven by the EF-TEM image shown in Figure 2a. The darker PDMS domain could clearly be differentiated from the light POEM domain due to the higher electron density of Si in PDMS compared to that of C, H, or O in POEM.[25] The PDMS-*g*-POEM comb copolymer had a well-defined micellar morphology consisting of an interior core of PDMS and an exterior shell of POEM. The distribution of micelle sizes of PDMS-*g*-POEM was bimodal with small cores with a diameter of ∼50 nm and large cores with a diameter of ∼200 nm for an average size of 130 nm. We attributed the presence of large micelles to the molecular weight distribution of the PDMS-*g*-POEM comb copolymer as well as consolidation of small micelles to minimize interfacial tension with ethanol by reducing the surface area in contact with ethanol. In other studies of amphiphilic block copolymers consisting of PDMS and PEO chains, spherical micelles, cylindrical micelles, and spherical microdomains dispersed in a continuous matrix have been reported in addition to uni- or multilamellar vesicles.[26−29] Micelle morphology is largely dependent on experimental parameters, such as the molecular weight of the polymers, relative chain length ratio of each block, type of medium, and concentration. The shape and size of the PDMS-*g*-POEM comb copolymer with a molecular weight of 14000 g mol^{-1} in ethanol (1 wt %) are comparable to those reported by Wang et al.;[29] these authors reported that a $POEGMA_{11.6}$−$PDMS_{11}$−$POEGMA_{11.6}$ triblock copolymer with a molecular weight of 9400 g mol^{-1} could self-assemble into spherical single micelles with a diameter of ∼100 nm in aqueous solution (0.5 mg mL^{-1}). However, it should be noted that comb copolymers are easier to synthesize and cheaper than block copolymers.[30−32]

The thermal stability and degradation of the PDMS-*g*-POEM comb copolymer was examined by TGA analysis under a constant flow rate of N_2 and air as shown in Figure 2b. The minor decrease (<2%) in thermal stability below 100 °C was caused by the removal of H_2O bound weakly to the polymer. Under N_2 flow, thermal degradation started at the onset temperature of 286 °C (after 5% decomposition) and then sharply accelerated in the temperature range of 300−400 °C. At

DOI: 10.1021/acsami.5b01010
ACS Appl. Mater. Interfaces 2015, 7, 7767−7775

temperatures higher than 600 °C, <7% of carbon and ceramic residues derived from the PDMS domain remained. In contrast, under air flow, the onset temperature was 207 °C, and PDMS-*g*-POEM thermally decomposed faster due to additional O_2-driven oxidation of the polymer. However, the percentage of residues under air was slightly higher than that under N_2, because the inorganic component (Si) of the PDMS domain was converted to oxygen-containing oxide (SiO_2) under the air environment. The glass transition temperature (T_g) of PDMS and POEM was reported to be −136 and −66 °C, respectively, indicating a rubbery state of the PDMS-*g*-POEM comb copolymer.[28]

Formation of Well-Organized Meso-Macroporous TiO_2/SiO_2 Films. Well-ordered meso-macroporous TiO_2/SiO_2 mixed oxide thin films with high porosity, large pores, and good interconnectivity were prepared using the PDMS-*g*-POEM comb copolymer and TTIP as a structure-directing agent and titania precursor, respectively, as observed by SEM in Figure 3a−c. The diameter of the pores was ∼100 nm with a

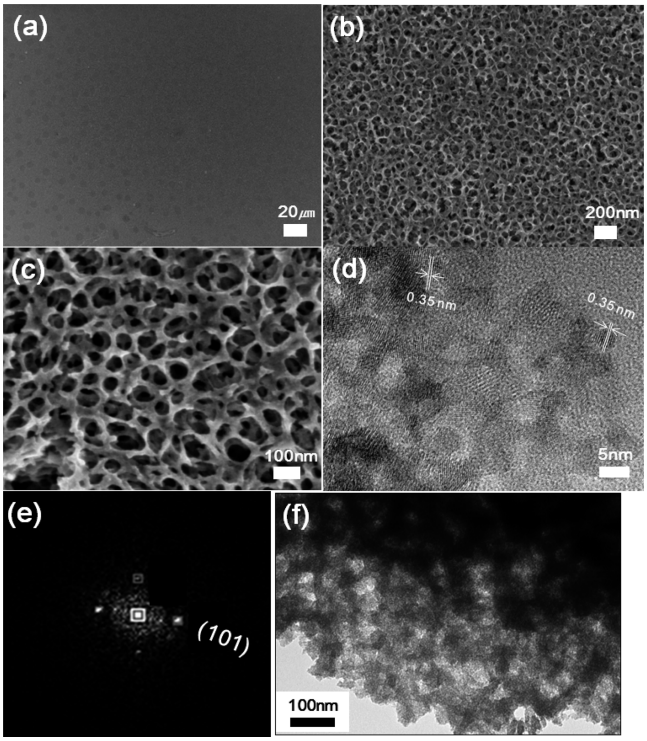

Figure 3. Well-organized meso-macroporous TiO_2/SiO_2 films derived from PDMS-*g*-POEM comb copolymer; SEM images at (a) low, (b) medium, and (c) high magnifications, and (d) HRTEM image, (e) SAED pattern, and (f) TEM image.

distribution from 50 to 115 nm, indicating that pore size falls between the mesoporous and macroporous ranges. Average wall thickness between pores was ∼20 nm. More importantly, the ordering of the meso-macroporous structure spanned a long length scale (i.e., 5 cm × 5 cm) without macroscopic cracks as revealed by SEM images taken at low magnification. The pore size of the films (∼100 nm) was comparable to that of the cores of micelles (∼130 nm) in the TEM image shown in Figure 2a, indicating that PDMS-*g*-POEM is a robust structure-directing agent. It is well-known that only core domains form pores after removing the micelles template.[37] Thus, the slightly smaller size of the pores than the cores of micelles is due to slight thermal shrinkage of the metal oxide skeleton during thermal treatment as a result of the selective incorporation of TTIP in the POEM shell of micelles and the conversion of TTIP and PDMS to TiO_2 and SiO_2, respectively. The HRTEM and its selected-area electron diffraction (SAED) pattern revealed that the framework of the thin film consisted of anatase nanocrystallites as shown in Figure 3d and e. The *d*-spacing was determined to be ∼0.35 nm, which is consistent with the results of the XRD pattern. The XRD pattern of the meso-macroporous TiO_2/SiO_2 film on FTO glass is shown in Figure S1 in the Supporting Information. Relatively weak peaks at 25.3° and 64.5° were assigned to the (101) and (204) planes of anatase TiO_2 (JDPDS Card No. 21−1272), respectively. We attributed the sharp peaks to SnO_2 in the FTO substrate. SiO_2 crystallites were not observed due to the low concentration of SiO_2 in the thin film and the amorphous nature of SiO_2.[15−18] The morphology and pore structures of the TiO_2/SiO_2 mixed oxide thin film were also confirmed by the TEM image shown in Figure 3f; there was good agreement between the TEM and SEM observations.

A plausible mechanism for the formation of well-organized meso-macroporous structures is the cooperative assembly of TTIP and PDMS-*g*-POEM micelles as depicted in Scheme 2. The EISA process coupled with sol−gel chemistry involves four stages: (1) evaporation of solvent in the sol−gel solution to induce self-assembly, (2) equilibrium of solvent with the environment, (3) meso-structuration of the inorganic−organic hydrid, and (4) condensation to form a porous network after thermal treatment.[33] The selective, preferential interaction between TTIP and POEM chains allowed the intermediate products of TTIP to stay in the hydrophilic POEM domains during the sol−gel process. However, the hydrophobic PDMS domain tended to strongly repel the ethanol and intermediate products of TTIP via the good−poor solvent pair effect. As a result, the evaporation of ethanol induced micelle formation with random close packing and intermicellar arrangement as a form of the continuous POEM/TTIP matrix with a dispersed spherical PDMS domain in the organic−inorganic hybrid film. The hydrophobic PDMS core served as a porogen, leaving spherical empty spaces in the TiO_2 frame after thermal decomposition into gaseous products (i.e., CO_2 and H_2O) at 450 °C under air. At the same time, the PDMS domain functioned as a SiO_2 source to alleviate distortional stress to the TiO_2 framework as a result of thermal shrinkage upon calcination.[34−36] The POEM domain was also burnt out during annealing process but provided space for TTIP to convert to TiO_2 inorganic walls. In this study, the average molecular weight of PDMS-*g*-POEM comb copolymer was ∼14400 g/mol with a PDMS/POEM ratio of 1:1.5. Using comb copolymers with a larger molecular weight and higher PDMS content will lead to the formation of much larger pores.

To study the property−structure relationship and effect of TTIP on the morphology of the TiO_2/SiO_2 thin film, we investigated TTIP amounts of 0.025, 0.075, 0.1, and 0.15 mL, corresponding to molar ratios of TTIP to PDMS-*g*-POEM of 0.009, 0.027, 0.04, and 0.05, respectively. At a molar ratio of TTIP to polymer of 0.009, the skinny film skeleton collapsed and disconnected walls were observed despite rough meso-macroporous structure retention (Figure 4a). A thin film with well-defined mesoporosity was obtained when the molar ratio of TTIP to polymer was 0.027 (Figure 4b). As the amount of TTIP increased, the pore size decreased gradually to ∼50 nm (Figure 4c). Only a dense thin film with almost complete

DOI: 10.1021/acsami.5b01010
ACS Appl. Mater. Interfaces 2015, 7, 7767−7775

Scheme 2. Mechanism for the Formation of Well-Organized Meso-Macroporous TiO_2/SiO_2 Films Using PDMS-*g*-POEM Comb Copolymer as a Structure-Directing Agent

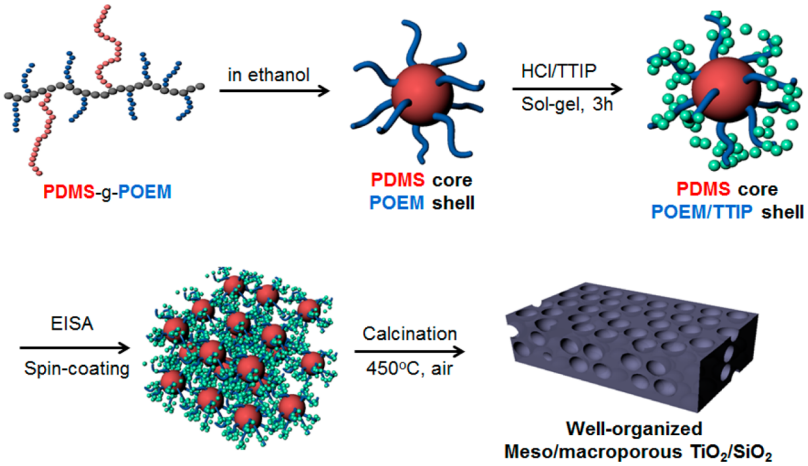

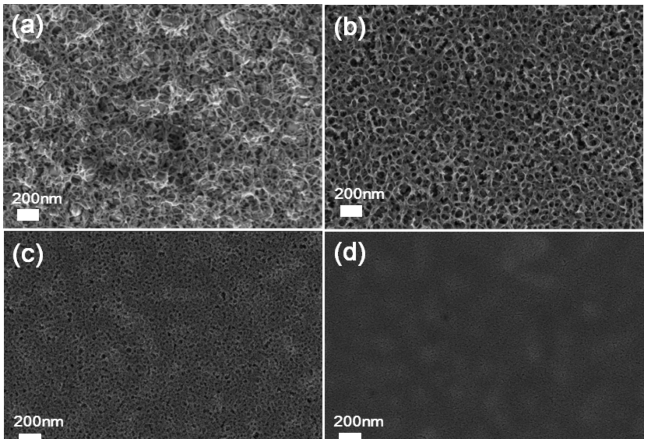

Figure 4. SEM images of meso-macroporous TiO_2/SiO_2 films with various amounts of TTIP: (a) 0.025 mL, (b) 0.075 mL, (c) 0.1 mL, and (d) 0.15 mL.

blockage of all pores was observed at an extremely high concentration of TTIP (Figure 4d), indicating that the ratio of inorganic precursor to polymer template plays a pivotal role in controlling pore structure and film morphology.

The SEM images in Figure 5 demonstrate the effect of polymer concentration on the morphology of meso-macroporous TiO_2/SiO_2 thin films. Polymer concentration did not affect the mesostructure and morphology of films as significantly as the TTIP/polymer ratio (Figure 4). However, the number of vertically perforated pores increased as the polymer concentration increased. This is because the density of micelles per unit volume of solution at higher polymer concentrations was high enough for micelles to come closer and stack more regularly/orderly in a three-dimensional array than at lower concentrations of polymer. The increase in concentration of the polymer solution had an obvious effect on the formation of large micron-sized cracks as shown in Figure S2 in the Supporting Information. When the polymer concentration reached 20%, star-shaped large cracks >10 μm in size appeared because the film was not strong enough to endure thermal shrinkage stress due to the high film thickness.

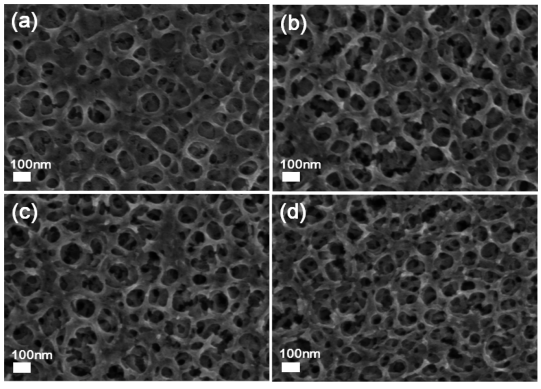

Figure 5. SEM images of meso-macroporous TiO_2/SiO_2 films with various concentrations of polymer solution: (a) 3%, (b) 10%, (c) 15%, and (d) 20%.

The effect of sonication on the film morphology was also investigated, and the results are shown in Figure S3 in the Supporting Information. In particular, a 2 h sonication treatment was applied to polymeric sol–gel solutions before spin-coating the solutions on a glass substrate under the same conditions as used in the other experiments.[38] Micelles with an average core diameter of 100 nm were broken down into smaller polydispersed micelles, and the pore diameter of the films decreased to ~30 nm. A relatively less-defined meso-macroporous structure was observed, indicating that sonication treatment had a negative effect on pore generation.

Additionally, a poorly structured meso-macroporous thin film with dense aggregated areas was formed when HCl was not used as shown in Figure S4 in the Supporting Information. HCl is a well-known catalyst for hydrolysis, and thus the addition of HCl in the sol–gel process accelerates the formation of Ti–OH rather than Ti–OPr and retards the condensation process. The slow rate of condensation prevents TiO_2 from being formed abruptly in an uncontrolled way and gives enough time for the TTIP precursor to interact with the POEM domain via a secondary bonding interaction. This indicates that HCl is also one of the important factors in generating a well-defined meso-macroporous structure. A variety of solvents, such as methanol, isopropyl alcohol, chloroform, toluene, and tetrahydrofuran, have also been used to prepare the TiO_2/SiO_2 films as shown in Figure S5 in the Supporting Information. The results revealed that the ethanol-based process is the most effective in

DOI: 10.1021/acsami.5b01010
ACS Appl. Mater. Interfaces 2015, 7, 7767–7775

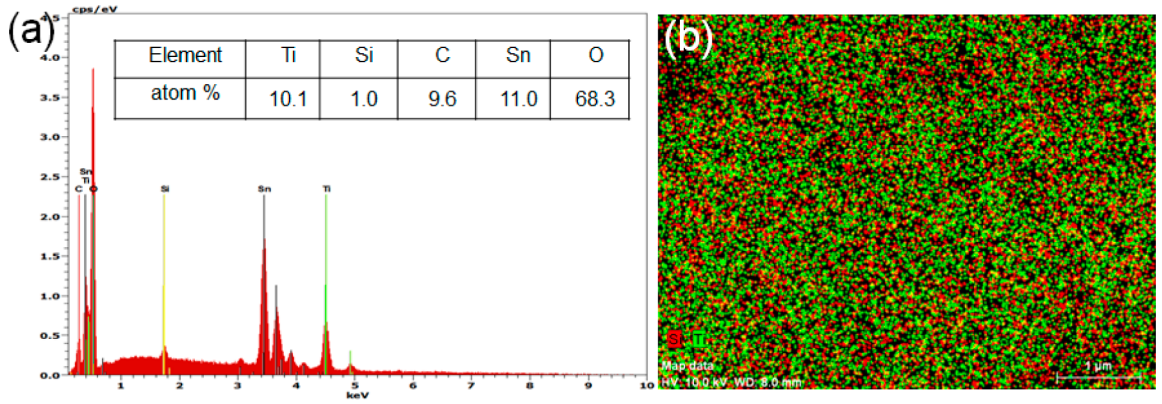

Figure 6. (a) EDS X-ray spectrum and (b) mapping of elements in the meso-macroporous TiO_2/SiO_2 thin film derived from the PDMS-*g*-POEM comb copolymer.

generating an organized meso-macroporous structure with good uniformity.

Elemental analysis of well-organized meso-macroporous TiO_2/SiO_2 films was performed based on the EDS spectrum shown in Figure 6. As discussed above, the TTIP precursor and PDMS chain functioned as sources of titanium (Ti) and silicon (Si), respectively. The atomic percentages of Ti and Si were approximately 10.1 and 1.0 at%, respectively, confirming the formation of mixed oxides with TiO_2 major and SiO_2 minor components. The high atomic percentage of carbon was due to residues from incompletely oxidized organic compounds. A meso-macroporous TiO_2/SiO_2 film prepared at a polymer concentration of 10% had a thickness of 600 nm, and the mesoporosity remained intact even in cross-section as shown in Figure S6 in the Supporting Information. Because the penetration depth of X-ray probes is approximately a few micrometers, tin (Sn) was detected from SnO_2 in the fluorine-doped tin oxide (FTO) substrate, which was used for future applications of the films in dye-sensitized solar cells (DSSCs). Elemental mapping of the film demonstrated that SiO_2 was uniformly dispersed and distributed throughout the TiO_2 matrix, confirming a well-mixed TiO_2/SiO_2 structure.

To examine the chemical environment of Si derived from the PDMS-*g*-POEM template in the film, we conducted XPS measurements, and the results are presented in Figure S7 in the Supporting Information. The binding energy of $Ti_{2p\ 3/2}$ corresponded to Ti in TiO_2 with the centroid of the peak at 459.2 eV. However, the binding energy of Si_{2p} was located at 102.8 eV, which corresponds to Si in SiO_2, not PDMS.[39,40] The O_{1s} spectrum had a sharp zenith at 530.7 eV and a broad shoulder peak at 532.4 eV, which we assigned to the oxygen in O−Ti−O and O−Si−O, respectively.[40] The PDMS ($(CH_3)_2$-Si-O) unit) domain in PDMS-*g*-POEM was directly converted to ceramic SiO_2 via thermal treatment and functioned as a structural supporter of the meso-macroporous TiO_2 structure. XPS analysis of carbon in the film revealed two peaks at 289.2 and 285.1 eV, which we attributed to the C−/C−H bond from residual carbons and O−C═O from chemically adsorbed CO_2 on the surface of the film. Therefore, we concluded that the meso-macroporous TiO_2/SiO_2 films derived from the PDMS-*g*-POEM comb copolymer were composed of anatase TiO_2, evenly distributed amorphous SiO_2, and residual carbons based on EDS, XRD, and XPS analyses.

The photocatalytic efficiency of the meso-macroporous TiO_2/SiO_2 thin film was measured, and the results are presented in Figure 7. Methyl orange (MO) has two

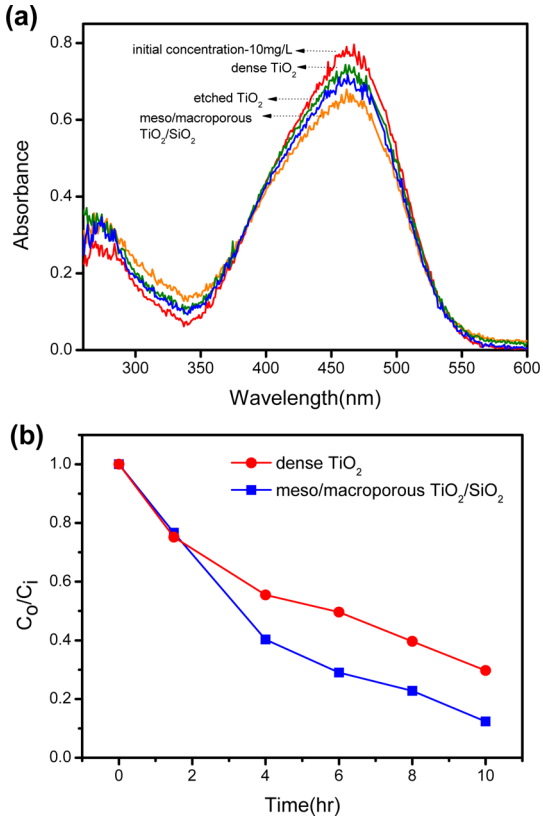

Figure 7. (a) UV−vis spectra of the initial concentration of MO and photodegraded MO by 600-nm-thick photocatalytic films after 1 h illumination, and (b) photodegration of methyl orange by 1-μm-thick photocatalytic films as a function of time.

characteristic peaks: a small peak at 260 nm and an intense peak at 467 nm. Photodegradation of MO into CO_2, H_2O, and salts (SO_4^{2-}, NO_3^-) by UV-illuminated TiO_2 results in decolouration of the MO dye solution due to destruction of the azo band (-N═N-) in MO and a decrease in the UV absorbance peak intensity of MO.[41,42] In parallel, the slight drift in the curve of the meso-macroporous TiO_2/SiO_2 thin film in the wavelength range from 290 to 350 nm is because of UV absorption of some intermediates started from the MO.[41] The lowest peak intensity at 467 nm obtained when using meso-macroporous TiO_2/SiO_2 thin film as a catalyst indicated that this film had a higher photodegradation rate than silica-etched

DOI: 10.1021/acsami.5b01010
ACS Appl. Mater. Interfaces 2015, 7, 7767−7775

TiO_2 and dense TiO_2 films. The photobleaching efficiency of silica-etched TiO_2 was better than that of dense TiO_2. Nevertheless, the dense TiO_2 film possesses a compact surface without any specific meso-macropores (the underlying structure comes from the FTO substrate) as shown in the SEM images in Figure S8a and b in the Supporting Information. The silica-etched TiO_2 film had a porous structure based on the SEM images shown in Figure S8s and d in the Supporting Information, and the successful removal of the SiO_2 component by NaOH was confirmed by elemental quantitative analysis using EDS in Figure S9 in the Supporting Information. When using 1-μm-thick photocatalytic films prepared by layer-by-layer deposition, MO was almost completely decomposed in the presence of the meso-macroporous TiO_2/SiO_2 thin film after 10 h of irradiation with UV light (Figure 7b, Figure S10 in the Supporting Information).

We attributed the enhanced MO dye degradation by the meso-macroporous TiO_2/SiO_2 thin film to the synergistic effect of a well-organized meso-macroporous structure and hybridization of TiO_2/SiO_2. It is important for porous structures to have a large surface area and offer high accessibility to guest molecules to result in enhancement of chemical reactions.[43,44] The well-organized meso-macroporous structure facilitated mass transfer of MO molecules deep inside the TiO_2/SiO_2 thin film and provided a larger surface area with a greater possibility of MO attack by a greater number of oxidizing agents (e.g., positive holes (h^+_{VB}) in the valence band and hydroxyl radicals (•OH) formed between holes as well as active OH^- groups on the surfaces of TiO_2 or H_2O) and reducing agents (e.g., conduction band electrons (e^-_{CB}) and the superoxide radical anion ($O_2^{\bullet-}$) produced by the reaction of O_2 adsorbed on the TiO_2 surface or dissolved in water as well as photogenerated electrons).[41,42] Additionally, the presence of SiO_2 in the vicinity of TiO_2 improves the efficiency of photobleaching because SiO_2, as an adsorbent for organic dyes, supplies concentrated organic dyes in the vicinity of the TiO_2 photoactive center and blocks the recombination of photogenerated holes and electrons from TiO_2, despite the poor photoactivity of SiO_2.[15−19] Furthermore, our meso-macroporous TiO_2/SiO_2 mixed oxides were prepared in the form of thin films tightly anchored on glass supports, which allows easy regeneration and simple recovery with no need for a tedious separation process such as that required for conventional powder catalysts.

CONCLUSIONS

A well-organized meso-macroporous TiO_2/SiO_2 thin film with high porosity and good connectivity was developed via the sol−gel process using an organized PDMS-*g*-POEM amphiphilic rubbery graft copolymer as a structure-directing agent in the absence of Si inorganic precursor. Amphiphilic PDMS-*g*-POEM copolymer was synthesized from two different monomethacylate-terminated macromonomers via free radical polymerization, which is a cheap and easy method to synthesize polymer. XRD analysis revealed that the PDMS-*g*-POEM comb copolymer was a structureless, randomly moving coil state with high mobility that was effective at interacting with the metal oxide precursor to form thin films. As a result, PDMS-*g*-POEM comb copolymer self-assembled in polar solvents, such as ethanol, into micelles with a uniform spherical morphology. The pore diameter of the thin film and wall thickness were controllable by varying the inorganic precursor to polymer ratio, polymer concentration in solution, sonication pretreatment, and HCl content. The well-organized meso-macroporous TiO_2/SiO_2 film showed greater photodegradation efficiency than the dense TiO_2 film and SiO_2-etched TiO_2 film, indicating the importance of a well-organized structure and SiO_2 doping for photocatalysis. The well-organized meso-macroporous TiO_2/SiO_2 film described here is simple to recover, as no tedious separation process is required, and is easy to regenerate.

ASSOCIATED CONTENT

Supporting Information

Low magnification SEM images of meso-macroporous TiO_2/SiO_2 films, SEM images of TiO_2/SiO_2 films after sonication treatment for 2 h, SEM images of TiO_2/SiO_2 films prepared without HCl, cross-sectional SEM image of the TiO_2/SiO_2 thin film, XRD patterns of bare FTO, and meso-macroporous TiO_2/SiO_2 on FTO and EDS of a silica-etched TiO_2 film. This material is available free of charge via the Internet at http://pubs.acs.org.

AUTHOR INFORMATION

Corresponding Author

*E-mail: jonghak@yonsei.ac.kr. Phone: +82-2-2123-5757. Fax: +82-2-312-6401.

Notes

The authors declare no competing financial interest.

ACKNOWLEDGMENTS

This work was supported by the National Research Foundation (NRF) (Grant NRF-2014K2A1B8047524), the Center for Advanced Meta-Materials (CAMM) (2014M3A6B3063716), and the Korea Center for Artificial Photosynthesis (KCAP) (2009-0093883).

REFERENCES

(1) Kresge, C. T.; Leonowicz, M. E.; Roth, W. J.; Vartuli, J. C.; Beck, J. S. Ordered Meso-macroporous Molecular Sieves Synthesized by a Liquid-Crystal Template Mechanism. *Nature* **1992**, *359*, 710−712.

(2) Peng, S.; Li, L.; Tan, H.; Cai, R.; Shi, W.; Li, C.; Mhaisalkar, S. G.; Srinivasan, M.; Ramakrishna, S.; Yan, Q. Hollow Spheres: MS_2 (M = Co and Ni) Hollow Spheres with Tunable Interiors for High-Performance Supercapacitors and Photovoltaics. *Adv. Funct. Mater.* **2014**, *24*, 2155−2162.

(3) Benehkohal, N. P.; Demopoulos, G. P. Green-Engineered All-Substrate Meso-macroporous TiO_2 Photoanodes with Superior Light-Harvesting Structure and Performance. *ChemSusChem* **2014**, *7*, 813−821.

(4) Colella, S.; Orgiu, E.; Bruder, I.; Liscio, A.; Palermo, V.; Bruchmann, B.; Samorì, P.; Erk, P. Titanium Dioxide Meso-macroporous Electrodes for Solid-State Dye-Sensitized Solar Cells: Cross-Analysis of the Critical Parameters. *Adv. Energy Mater.* **2014**, *4*, 1301362.

(5) Shan, G. B.; Assaaoudi, H.; Demopoulos, G. P. Enhanced Performance of Dye-Sensitized Solar Cells by Utilization of An External, Bifunctional Layer Consisting of Uniform β-$NaYF_4$:Er^{3+}/Yb^{3+} Nanoplatelets. *ACS Appl. Mater. Interfaces* **2011**, *3*, 3239−3243.

(6) Ahn, S. H.; Chi, W. S.; Park, J. T.; Koh, J. K.; Roh, D. K.; Kim, J. H. Direct Assembly of Preformed Nanoparticles and Graft Copolymer for the Fabrication of Micrometer-Thick, Organized TiO_2 Films: High Efficiency Solid-State Dye-Sensitized Solar Cells. *Adv. Mater.* **2012**, *24*, 519−522.

(7) Colodrero, S.; Forneli, A.; Lopez-Lopez, C.; Pelleja, L.; Miguez, H.; Palomares, E. Efficient Transparent Thin Dye Solar Cells Based on Highly Porous 1D Photonic Crystals. *Adv. Funct. Mater.* **2012**, *22*, 1303−1310.

DOI: 10.1021/acsami.5b01010
ACS Appl. Mater. Interfaces 2015, 7, 7767−7775

(8) Park, J. T.; Prosser, J. H.; Ahn, S. H.; Kim, S. J.; Kim, J. H.; Lee, D. Enhancing the Performance of Solid-State Dye-Sensitized Solar Cells Using a Meso-macroporous Interfacial Titania Layer with a Bragg Stack. *Adv. Funct. Mater.* **2013**, *23*, 2193−2200.
(9) Brinker, C. J.; Lu, Y.; Sellinger, A.; Fan, H. Evaporation-Induced Self-Assembly: Nanostructures Made Easy. *Adv. Mater.* **1999**, *11*, 579−585.
(10) Fan, J.; Boettcher, S. W.; Stucky, G. D. Nanoparticle Assembly of Ordered Multicomponent Mesostructured Metal Oxides via A Versatile Sol−Gel Process. *Chem. Mater.* **2006**, *18*, 6391−6396.
(11) Cheng, Y.-J.; Gutmann, J. S. Morphology Phase Diagram of Ultrathin Anatase TiO_2 Films Templated by a Single PS-*b*-PEO Block Copolymer. *J. Am. Chem. Soc.* **2006**, *128*, 4658−4674.
(12) Bastakoti, B. P.; Ishihara, S.; Leo, S. Y.; Ariga, K.; Wu, K. C.-W.; Yamauchi, Y. Polymeric Micelle Assembly for Preparation of Large-Sized Meso-macroporous Metal Oxides with Various Compositions. *Langmuir* **2014**, *30*, 651−659.
(13) Li, Y.; Bastakoti, B. P.; Imura, M.; Hwang, S. M.; Sun, Z.; Kim, J. H.; Dou, S. X.; Yamauchi, Y. Synthesis of Meso-macroporous TiO_2/SiO_2 Hydrid Films as An Efficient Photocatalysis by Polymeric Micelle Assembly. *Chem.—Eur. J.* **2014**, *20*, 6027−6032.
(14) Fattakhova-Rohlfing, D.; Wark, M.; Brezesinski, T.; Smarsly, B. M.; Rathouský, J. Highly Organized Meso-macroporous TiO_2 Films with Controlled Crystallinity: A Li-Insertion Study. *Adv. Funct. Mater.* **2007**, *17*, 123−132.
(15) Anderson, C.; Bard, A. J. An Improved Photocatalyst of TiO_2/SiO_2 Prepared by a Sol-Gel Synthesis. *J. Phys. Chem.* **1995**, *99*, 9882−9885.
(16) Anderson, C.; Bard, A. J. Improved Photocatalytic Activity and Characterization of Mixed TiO_2/SiO_2 and TiO_2/Al_2O_3 Materials. *J. Phys. Chem. B* **1997**, *101*, 2611−2616.
(17) Yu, J.; Yu, J. C.; Zhao, Xi. The Effect of SiO_2 Addition on the Grain Size and Photocatalytic Activity of TiO_2 Thin Films. *J. Sol−Gel. Sci. Technol.* **2002**, *24*, 95−103.
(18) Xiea, C.; Xua, Z.; Yang, Q.; Xue, B.; Du, Y.; Zhang, J. Enhanced Photocatalytic Activity of Titania−Silica Mixed Oxide Prepared via Basic Hydrolyzation. *Mater. Sci. Eng., B* **2004**, *112*, 34−41.
(19) Zeleňák, V.; Hornebecq, V.; Mornet, S.; Schäf, O.; Llewellyn, P. Meso-macroporous Silica Modified with Titania: Structure and Thermal Stability. *Chem. Mater.* **2006**, *18*, 3184−3191.
(20) Kim, D. J.; Kim, S. J.; Roh, D. K.; Kim, J. H. Synthesis of Low-Cost, Rubbery Amphiphilic Comb-Like Copolymers and Their Use in the Templated Synthesis of Meso-macroporous TiO_2 Films for Solid-State Dye-Sensitized Solar Cells. *Phys. Chem. Chem. Phys.* **2013**, *15*, 7345−7353.
(21) Bicerano, J. *Prediction of Polymer Properties*, 2nd ed.; Marcel Dekker Inc: New York, 1996.
(22) Roh, D. K.; Kim, S. J.; Jeon, H.; Kim, J. H. Nanocomposites with Graft Copolymer-Templated Meso-macroporous $MgTiO_3$ Perovskite for CO_2 Capture Applications. *ACS Appl. Mater. Interfaces* **2013**, *5*, 6615−6621.
(23) Ahn, S. H.; Park, J. T.; Kim, J. H.; Ko, Y.; Hong, S. U. Nanocomposite Membranes Consisting of Poly(vinyl chloride) Graft Copolymer and Surface-Modified Silica Nanoparticles. *Macromol. Res.* **2011**, *19*, 1195−1201.
(24) Luo, Z.; He, T.; Yu, H.; Dai, L. A Novel ABC Triblock Copolymer with Very Low Surface Energy: Poly(dimethylsiloxane)-block-Poly(methyl methacrylate)-block-Poly(2,2,3,3,4,4,4-heptafluorobutyl methacrylate). *Macromol. React. Eng.* **2008**, *2*, 398−406.
(25) Ahn, S. H.; Koh, J. H.; Seo, J. A.; Kim, J. H. Structure Control of Organized Meso-macroporous TiO_2 Films Templated by Graft Copolymers for Dye-sensitized Solar Cells. *Chem. Commun.* **2010**, *46*, 1935−1937.
(26) Rheingans, O.; Hugenberg, N.; Harris, J. R.; Fischer, K.; Maskos, M. Nanoparticles Built of Cross-Linked Heterotelechelic, Amphiphilic Poly(dimethylsiloxane)-b-poly(ethylene oxide) Diblock Copolymers. *Macromolecules* **2000**, *33*, 4780−4790.
(27) Kickelbick, G.; Bauer, J.; Huesing, N.; Andersson, M.; Holmberg, K. Aggregation Behavior of Short-Chain PDMS-*b*-PEO Diblock Copolymers in Aqueous Solutions. *Langmuir* **2003**, *19*, 10073−10076.
(28) Trapa, P. E.; Won, Y.-Y.; Mui, S. C.; Olivetti, E. A.; Huang, B.; Sadoway, D. R.; Mayes, A. M.; Dallek, S. Rubbery Graft Copolymer Electrolytes for Solid-State, Thin-Film Lithium Batteries. *J. Electrochem. Soc.* **2005**, *152*, A1−A5.
(29) Wang, G.; Chen, M.; Guo, S.; Hu, A. Synthesis, Self-Assembly, and Thermosensitivity of Amphiphilic POEGMA-PDMS-POEGMA Triblock Copolymers. *J. Polym. Sci., Part A: Polym. Chem.* **2014**, *52*, 2684−2691.
(30) Roh, D. K.; Kim, S. J.; Chi, W. S.; Kim, J. K.; Kim, J. H. Dual-Functionalized Meso-macroporous TiO_2 Hollow Nanospheres for Improved CO_2 Separation Membranes. *Chem. Commun.* **2014**, *50*, 5717−5720.
(31) Ahn, S. H.; Kim, D. J.; Chi, W. S.; Kim, J. H. Hierarchical Double-Shell Nanostructures of TiO_2 Nanosheets on SnO_2 Hollow Spheres for High-Efficiency, Solid-State, Dye-Sensitized Solar Cells. *Adv. Funct. Mater.* **2014**, *24*, 5037−5044.
(32) Ahn, S. H.; Kim, D. J.; Chi, W. S.; Kim, J. H. One-Dimensional Hierarchical Nanostructures of TiO_2 Nanosheets on SnO_2 Nanotubes for High Efficiency Solid-State Dye-Sensitized Solar Cells. *Adv. Mater.* **2013**, *25*, 4893−4897.
(33) Sanchez, C.; Boissière, C.; Grosso, D.; Laberty, C.; Nicole, L. Design, Synthesis, and Properties of Inorganic and Hybrid Thin Films Having Periodically Organized Nanoporosity. *Chem. Mater.* **2008**, *20*, 682−737.
(34) Liu, Y. R. One-Pot Route to Synthesize Ordered Meso-macroporous Polymer/Silica and Carbon/Silica Nanocomposites Using Poly(dimethylsiloxane)−Poly(ethylene oxide) (PDMS−PEO) as Co-Template. *Microporous Mesoporous Mater.* **2009**, *124*, 190−196.
(35) Memesa, M.; Weber, S.; Lenz, S.; Perlich, J.; Berger, R.; Müller-Buschbaumc, P.; Gutmann, J. S. Intergrated Blocking Layers for Hybrid Organic Solar Cells. *Energy Environ. Sci.* **2009**, *2*, 783−790.
(36) Grégori, D.; Benchenaa, I.; Chaput, F.; Thérias, S.; Gardette, J.-L.; Léonard, D.; Guillard, C.; Parola, S. Mechanically Stable and Photocatalytically Active TiO_2/SiO_2 Hybrid Films on Flexible Organic Substrates. *J. Mater. Chem. A* **2014**, *2*, 20096−20104.
(37) Bastakoti, B. P.; Li, Y.; Kimura, T.; Yamauchi, Y. Asymmetric Block Copolymers for Supramolecular Templating of Inorganic Nanospace Materials. *Small* DOI: 10.1002/smll.201402573.
(38) Zhang, Y.; Li, H.; Liu, Y.-Q.; Wang, J. Sonochemical Synthesis and Liquid Crystal Assembly of PS-*b*-PEO−titania Aggregates. *Chem. Commun.* **2012**, *48*, 8538−8540.
(39) O'Hare, L.-A.; Parbhoo, B.; Leadley, S. R. Development of A Methodology for XPS Curve-Fitting of the Si 2p Core Level of Siloxane Materials. *Surf. Interface Anal.* **2004**, *36*, 1427−1434.
(40) Stakheev, A. Y.; Shpiro, E. S.; Apijok, J. XPS and XAES Study of TiO_2-SiO_2 Mixed Oxide System. *J. Phys. Chem.* **1993**, *97*, 5668−5672.
(41) Park, J. T.; Lee, C. S.; Kim, J. H. One-Pot Synthesis of Hierarchical Meso-macroporous SnO_2 Spheres Using a Graft Copolymer: Enhanced Photovoltaic and Photocatalytic Performance. *RSC Adv.* **2014**, *4*, 31452−31461.
(42) Yu, J.-G.; Yu, H.-G.; Cheng, B.; Zhao, X.-J.; Yu, J. C.; Ho, W.-K. The Effect of Calcination Temperature on the Surface Microstructure and Photocatalytic Activity of TiO_2 Thin Films Prepared by Liquid Phase Deposition. *J. Phys. Chem. B* **2003**, *107*, 13871−13879.
(43) Biswas, C. S.; Hazer, B. Synthesis and Characterization of Stereoregular Poly(*N*-ethylacrylamide) Hydrogel by Using $Y(OTf)_3$ Lewis Acid. *Colloid Polym. Sci.* **2015**, *293*, 143−152.
(44) Biswas, C. S.; Sulu, E.; Hazer, B. Effect of the Composition of Methanol−Water Mixtures on Tacticity of Poly(*N*-ethylacrylamide) Gel. *J. Appl. Polym. Sci.* **2015**, *132*, 41668−41678.

DOI: 10.1021/acsami.5b01010
ACS Appl. Mater. Interfaces 2015, 7, 7767−7775